Journal of Ocean Engneering and Technology, Vol. 2, No. 1, pp. 83~89, June, 1988

⊙ Technical Paper

Vortex Motion near the Edge of a Semi-Infinite Flat Plate Impulsively Started Transversally+

Y. K. Suh* and L. S. Seo*

(*Received April* 4, 1988)

急進하는 半無限 平板 주위의 보텍스 운동

徐 龍 權·徐 利 洙

Key Words : Vortex Motion(보텍스 운동), Discrete Vortex Model(분리 보텍스 모형), Single Vortex Model(단일 보텍스 모형), Kutta Condition(쿠타 조건), Circulation(순환)

초 록

정지된 유동장에 놓인 반무한 평판이 横方向으로 갑자기 출발하는 경우에 있어서 평판의 끝에서 발생하는 보텍스의 거동을 해석적 및 수치적 측면에서 검토하였다. 해석적 방법은 단일 보텍스 모델에 근거를 두었으며, 해석결과 순환량은 시간의 1/3승, 보텍스의 중심까지의 거리는 시간의 2/3승에 비례하여 증가함을 알 수 있었다. 룬게·쿠타(Runge-Kutta)方法을 써서 분리 보텍스 모델에 따른 비선형 운동방정식의 解를 수치적으로 구했다. 수치해는 시간의 경과에 따라 해석 解에 접근하였다. 보텍스의 형상에 있어서도 실험결과와 잘 맞았다.

1. Introduction

The discrete vortex model is emerging as a powerful method for simulating high-Reynolds-number flows of unsteady nature[1]. The first attempt to study the fluid motion by this was made by Rosenhead[2], who replaced the continuous two-dimensional vortex sheet by a collection of discrete point vortices. Early applications of this method to the unsteady motions of fluids around bluff bodies were made by Sarpkaya[3], Chaplin[4], Yang & Bar-lev[5], Stansby[6], Maull & Milliner[7] and Kuwahara[8], etc. All of these works were based on the straightforward method and resulted in the random chaotic motions of vortices in the flow field where they rolled up.

A significant step forward was made by Fink & Soh[9], who asserted that the chaotic nature was due to the logarithmic singularity. They introduced the so called 'rediscretization' technique by which every time the vortex is convected the position and the circulation of each vortex are rearranged. Using this method Fink & Soh demonstrated smooth roll-up calculations for a finite vortex sheet. The smoothness remained for much longer time than had been previously reported. Sarpkaya & Schoaff [10] utilized this technique in studying the vortex shedding around a circular cylinder, and showed

+ Presented at the 1987 KCORE Autumn Conference

* Member, Mechanical Engineering Dep't, Dong-A University

that a smoother development than the straightforward method was assured.

Recently Higdon & Pozrikidis [11] proposed a new scheme which combined the spectral method adopted by Merion, Baker & Orszag [12] and the rediscretization method. They applied this scheme to predict the motion of an initially circular vortex sheet and the motion of an initially flat vortex sheet with uniform circulation subject to a periodic disturbance in the circulation. They managed to estimate the accurate critical time at which the sheets locally exhibited an infinite number of vortex windings.

In the present paper, we apply the discrete vortex model in studying the motions of vortices around the edge of a semi-infinite flat plate impulsively started transversally. To avoid the complexity, the simple straightforward method is used in the numerics. An analytic solution is obtained by approximating the vortex sheet with a single vortex. While the single vortex model adopted here would not strictly describe the whole flow field accurately, the simplicity renders much of its analytic properties tractable.

2. Analysis by the Single Vortex Model

We consider a potential flow around a semi-infinite plate occupying the positive x-axis in the z-plane. To obtain the complex potential $w=\phi+i\psi$, we transform the z-plane to the ζ-plane with

$$z=\frac{1}{2}\zeta^2 \tag{1}$$

where $z=x+iy$, and $\zeta=\xi+i\eta$. Then it is clear that

$$w=\zeta \tag{2}$$

satisfying the impermeable condition on the body. The other multiplying constants which may appear in the equations (1) and (2) are meaningless since there is no charateristic scale for length or time.

Now we consider the viscous effect of the fluid from $t=0$, which is equivalent to the impulsive motion of the plate. Experimental evidence reveals that the spiral form of vortex sheet is generated near the edge of the plate for this case. First of all we replace the vortex sheet by a single point vortex with circulation Γ_s at $\zeta=\zeta_s$ in the ζ-plane equivalently at $z=z_s$ in the z-plane. Then the complex potential satisfying the condition on the boundary becomes

$$w=\zeta+\frac{i}{2\pi}\Gamma_s\ln\frac{\zeta-\zeta_s}{\zeta-\bar{\zeta}_s} \tag{3}$$

where $\bar{\zeta}_s$ represnts the poitin of the image vortex. The comlex velocity q is then

$$\bar{q}=\frac{dw}{dz}=\frac{dw}{d\zeta}\frac{d\zeta}{dz}=\frac{1}{\zeta}\left[1+\frac{i}{2\pi}\Gamma_s\left(\frac{1}{\zeta-\zeta_s}-\frac{1}{\zeta-\bar{\zeta}_s}\right)\right] \tag{4}$$

Next we introduce the Kutta condition at the edge so that the velocity of fluid particles at the point is bounded for $t>0$:

$$\Gamma_s=\frac{\pi s}{\cos\beta} \tag{5}$$

Where s and β are defined as $\zeta_s=s\exp(i\beta)$. The velocity at $\zeta=0$ is obtained as

$$q_0=\frac{i}{2\pi}\Gamma_s\left(\frac{1}{\zeta^2_s}-\frac{1}{\bar{\zeta}^2_s}\right)=\frac{i}{\pi}\Gamma_s\frac{\sin 2\beta}{s^2} \tag{6}$$

It is assumed that the vortex generated continuously at the edge adds to Γ_s. The rate at which the vortex circulation Γ_s is incresed is generally known as References (3), (4), (6) and (10).

$$\frac{d\Gamma_s}{dt}=-\frac{1}{2}|q_0|^2 \tag{7}$$

so that

$$\frac{d\Gamma_s}{dt}=-\frac{\Gamma_s^2\sin^2 2\beta}{2\pi^2 s^4} \tag{8}$$

In order to satisfy the momentum conservation, the total forces acting on the plate and the vortex must be zero[13], which yields

$$\frac{1}{\Gamma_s}\frac{d}{dt}(\Gamma_s z_s)=\frac{1}{\zeta_s}\left[1-\frac{i}{2\pi}\Gamma_s\left(\frac{1}{\zeta_s-\bar{\zeta}_s}\right)\right] \tag{9}$$

Similarity assumption in the present problem is equivalent to assuming $\beta=$const. by which we get $\Gamma_s\sim t^{1/3}$, $z_s\sim t^{2/3}$ using (5) and (8). Thus, the right hand side of (9) must vanish, or

$$\Gamma_s=4\pi s\cos\beta \tag{10}$$

Equations (5) and (10) are coupled to give

$$\beta=60^\circ \tag{11}$$

With this, (8) and one of (5) and (10) produce

$$s=\left(\frac{9}{4\pi}t\right)^{1/3} \tag{12}$$

$$\Gamma_s=2\pi\left(\frac{9}{4\pi}t\right)^{1/3} \tag{13}$$

In the z-plane,

$$r=\frac{1}{3}\left(\frac{9}{4\pi}t\right)^{2/3},\quad \delta_s=60^\circ \tag{14}$$

where r and δ_s are defined as $z_s=r\exp(i\delta_s)$. Note that $r\sim t^{2/3}$ and $\Gamma_s\sim t^{1/3}$. This nature was also found by Kaden[14] when he studied the roll-up of an initially straight semi-infinite vortex sheet. It is also interesting to note that his result

$$\delta_s=tan^{-1}\left(\frac{0.88}{0.57}\right)=57^\circ$$

is very close to (14).

3. Numerical Method Based on the Discrete Vortex Model

In this section, we replace the vortex sheet by a system of discrete vortices and apply the numerical method to follow their paths. The complex potential w and the complex velocity q are as follows;

$$w=\zeta+\frac{i}{2\pi}\sum_{k=1}^{m}\Gamma_k\ ln\frac{\zeta-\zeta_k}{\zeta-\bar{\zeta}_k} \tag{15}$$

$$\bar{q}=\frac{1}{\zeta}\left[1+\frac{i}{2\pi}\sum_{k=1}^{m}\Gamma_k\left(\frac{1}{\delta-\delta_k}-\frac{1}{\delta-\bar{\zeta}_k}\right)\right] \tag{16}$$

where Γ_k is the circulation of the k^{th} point vortex and ζ_k represents its position in the ζ-plane.

Next we consider the vortex generation at the edge of the plate. It is clear that at $t=0$ the velocitt at the edge is infinite so that $\frac{d\Gamma}{dt}\to\infty$ at that instant. To avoid this singularity, we fix the generation point at

$$\zeta=i\,h \tag{17}$$

Then the circulation Γ_n of new vortex generated at that point may be evaluated as

$$\Gamma_n=\frac{1}{2}\left|q\right|^2_{\zeta=ih}\Delta t \tag{18}$$

where Δt is time increment for each vortex generation.

Now we constitute the equation for the motions of point vortices. It can be shown that

$$\frac{d\bar{\zeta}_j}{dt}=\frac{1}{(\bar{\zeta}\bar{\zeta})_j}\left[1+\frac{i}{2\pi}\sum_{k\,1}^{m}\Gamma_k\left(\frac{1}{\zeta_j-\zeta_k}-\frac{1}{\zeta_j-\bar{\zeta}_k}\right)\right]$$

$$(j=1,2,\ m) \tag{19}$$

where $1/(\zeta_j-\zeta_k)$ should be omitted in summation if $j=k$. Equation (19) is highly non-linear. The numerical method such as the second order scheme

$$\bar{\zeta}^{(n)}=\bar{\zeta}_j{}^{(0)}+\delta t\left(\frac{d\bar{\zeta}_j}{dt}\right)^{(0)}+Q(\delta t^2) \tag{20}$$

where the superscripts (n) and (o) denote 'new' and 'old' respectively, or the fourth-order Runge-Kutta method may be applied. δt in (20) is time interval for vortex-advancement.

New vortices can be introduced into the flow field at the end of multiple of δt, say $\Delta t=n\delta t$; in this study $n=2$ is chosen as is usual.

It should be mentioned here that h introduced to avoid the singularity at the edge becomes now the length scale in the ζ-plane; thus, the time increment Δt as a time scale can be combined with h to produce a certain parameter out of equation (19). We put

$$\zeta=h\zeta^*,\quad t=(\Delta t)t^*,$$

$$q=\frac{1}{h}q^*,\quad \Gamma_k=\frac{\Delta t}{h^2}\Gamma_k^* \tag{21}$$

and substitute these into (19) to obtain

$$\frac{d\bar{\zeta}_j{}^*}{dt}=H_t\frac{1}{(\zeta^*\bar{\zeta}^*)_j}\left[1+\right.$$

$$\left.H_t\frac{i}{2\pi}\sum_{k=1}^{m}\Gamma_k^*\left(\frac{1}{\zeta_j{}^*-\zeta_k{}^*}-\frac{1}{\zeta_j{}^*-\bar{\zeta}_k{}^*}\right)\right]$$

$$(j=1,2,\cdots m) \tag{22}$$

where $H_t=\frac{t}{h^3}$ is the parameter. Hence, even if Δt and h are changed, solutions $\Gamma^*_k, q^*, \cdots$ are invariant if H_t is invariant, while $\Gamma_k. q, \cdots$ are evaluated by (21).

Calculation procedure is as follows. At the time level t, q at $\zeta=ih$ is evaluated through (16). A new vortex is introduced at $\zeta=ih$ with the circulation determined by (18). The new position of each vortex is obtained by (20) and the equivalent method. Above sequence is repeated till the final time level required.

4. Results and Discussions

Shown in Fig. 1 is development of vortices generated near the plate edge and covected in the flow field with $h=0.25$ and $\Delta t=0.02$. Here and afterwards, the fourth-order Runge-Rutta method is used for vortices-convection unless otherwise specified. It can be seen that as time elapses the system of

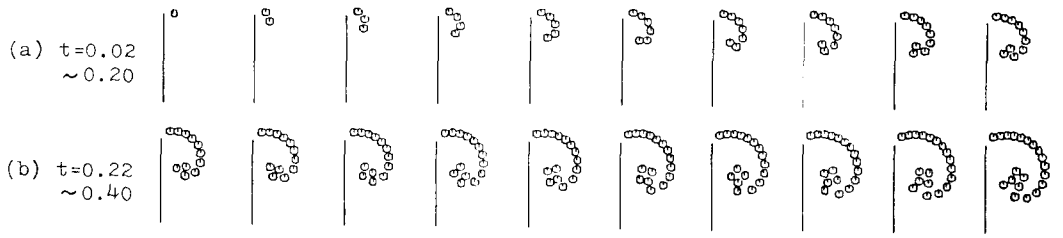

Fig. 1(a-b) For legend, see the next page

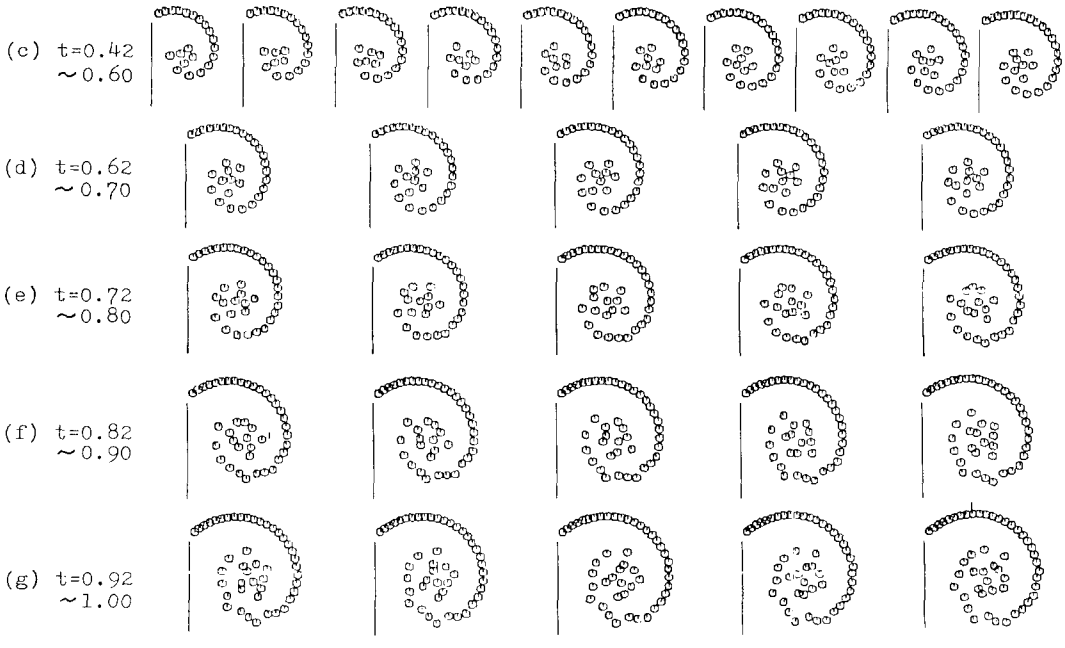

Fig. 1(c-g) Development of vortices near the edge of the plate: $h=0.25$, $\Delta t=0.02$

vortices take a similar form. The end point vortex (generated at $t=0$) starts to roll up continuously from $t=0.2$ when it seems to reveal singularity. This kind of singularity is charaterized as the endless winding of vortex sheet at that point[11]. We suspect that the time t when this singularity takes place tends to zero as Δt is decreased for fixed h, since the circulation of the end vortex is the largest. Comparison of three cases of $\Delta t=0.20$, 0.10, and 0.05 for $h=1.0$ supports this argument as shown in Fig. 2. We note that the end vortex for $\Delta t=0.05$ is severely distorted at $t=1.0$, while that for $\Delta t=0.10$ or 0.20 still stands on a smooth curve. It turned out that a similar distortion exists at $t=2.0$ for $\Delta t=0.10$ and at $t=4.0$ for $\Delta t=0.20$. In Fig. 3, vortices-arrangement for $\Delta t=0.05$ is compared with that for $\Delta t=0.20$ at $t=2.0$

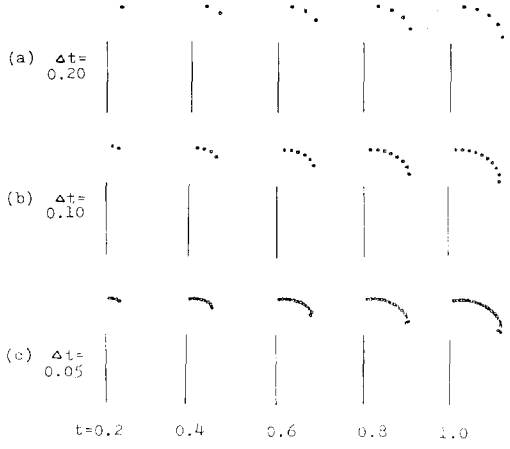

Fig. 2 Effect of Δt on the roll-up of discrete vortices. States at five time levels are shown. Special attention is to be paid to the movement of the end point-vortex $h=1.0$

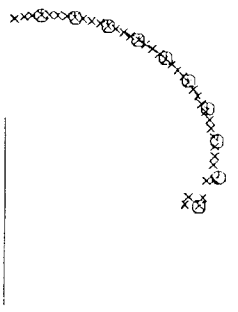

Fig. 3 Effect of Δt on the roll-up of discrete vortices. States at $t=1.0$ are shown for $h=1.0\times$, $\Delta t=0.05$; ⓣ, $\Delta t=0.20$

for $h=1.0$ to help understanding.

Fig. 4 shows the pattern of vortices at $t=1.0$ for three cases of $\Delta t=0.05$, 0.02, and 0.01 for $h=0.25$. They agree well near the plate edge, but not much in the core region, where effect of the size of Δt is great since each vortex during convection changes its direction sharply due to the end effect as is mentioned previously.

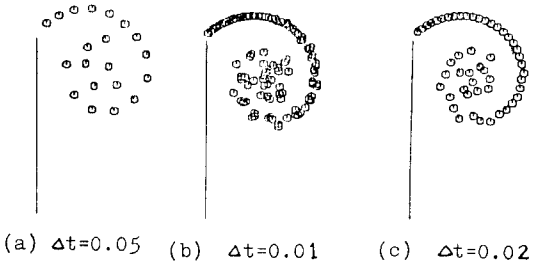

Fig. 4 Patterns of vortex sheets at $t=1.0$ for three cases of Δt, $h=0.25$

The second order scheme (20) is also used for convection. In Fig. 5 compared is the result by the fourth-order Runge-Kutta method with that by (20). They also agree well near the edge, but not in the core region, where the second order scheme reveals smoother arrangement in array of vortices than the other. This smoother pattern is of course rather erroneous by the reason discussed in connection with Fig. 2.

The similarity nature represented by the parameter H_t is studied. Fig. 6 is a plot of vortex pattern for two cases of same $H_t=0.2$. Since h is

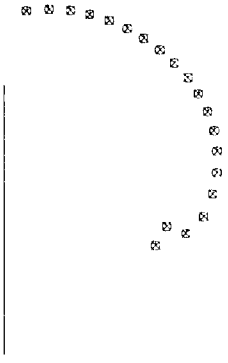

Fig. 6 Distributions of point vortices after 20 vortices are generated for $H_t=0.20$. ⓣ, $h=1.0$, $\Delta t=0.2$; ×, $h=2.0$, $\Delta t=1.6$. The scale used in plotting ⓣ is 4 times larger than that for ×

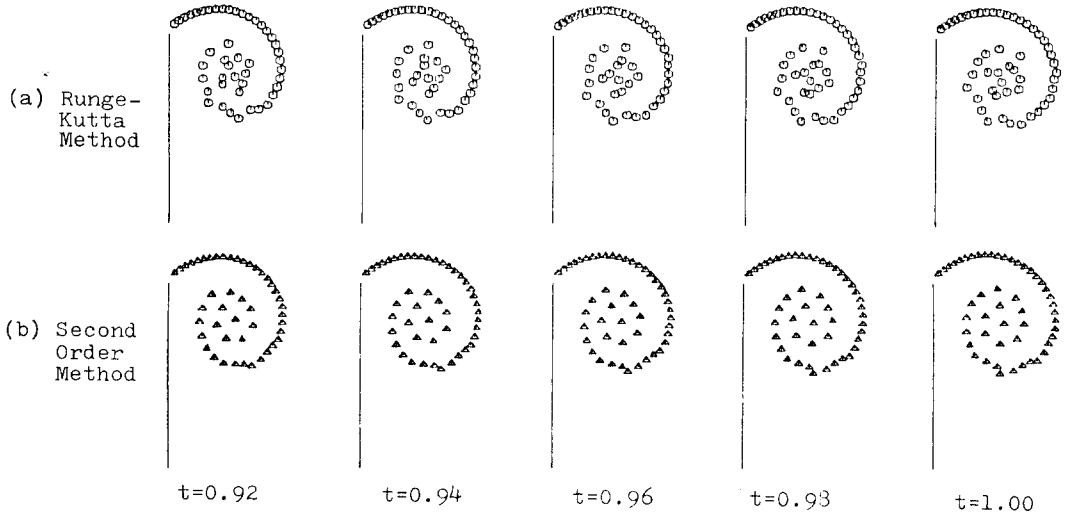

Fig. 5 Development of point vortices during $0.92\leq t\leq 1.00$ by two methods. $h=0.25$, $\Delta t=0.02$

increased twice, the reduced scale used in plotting the one for larger h is 4 based on (21) and (1). As is analysed, two patterns are identified.

The numerical solution based on the discrete vortex model is compared with the analytic solution for the single vortex model represented in section 2. Fig. 7 compares Γ_s of (13) with Γ_0 where

$$\Gamma_0=\sum_{k=1}^{m}\Gamma_k \tag{23}$$

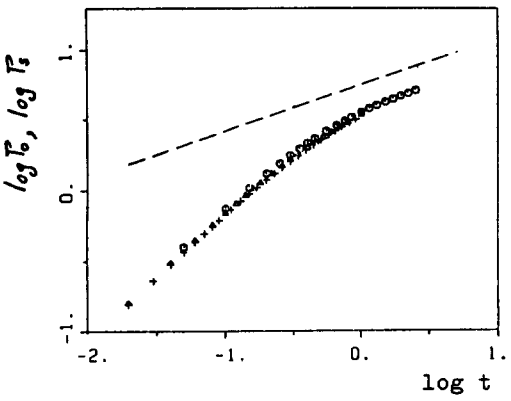

Fig. 7 Circulations versus time in log-log scales. Γ_s by theory (13); Various symbols are numerical results of Γ_0 by (23) for $h=0.25$. ○, $\Delta t=0.05$; △ $\Delta t=0.02$; +, $\Delta t=0.01$

is the numerical result. It is seen that although the starting vortex has circulation much lower than theory, Γ_0 tends to Γ_s asymptotically for large t. Fig. 8 compares r of (14) with r_o where

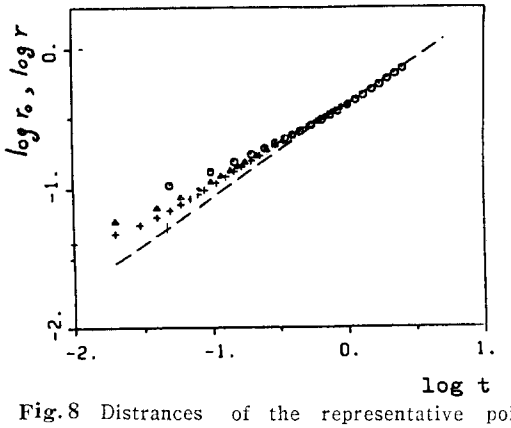

Fig. 8 Distrances of the representative point vortices from the the plate edge. ··· r by theory (14); Symbols are numerical results of r by (24) for $h=0.25$. See the caption of Fig. 7 for classifications

$$r_o=\left|\frac{\sum_{k=1}^{m}\Gamma_k z_k}{\sum_{k=1}^{m}\Gamma_k}\right| \tag{24}$$

is the numerical result. In this figure, the descrete vortex model agrees very well with the single vortex model. Even for largest Δt, the two results coincide near $t=1.0$. Fig. 9 compares δ_s of (14) with δ_o where

$$\delta_o=\arg\left(\sum_{k=1}^{m}\Gamma_k z_k\right) \tag{25}$$

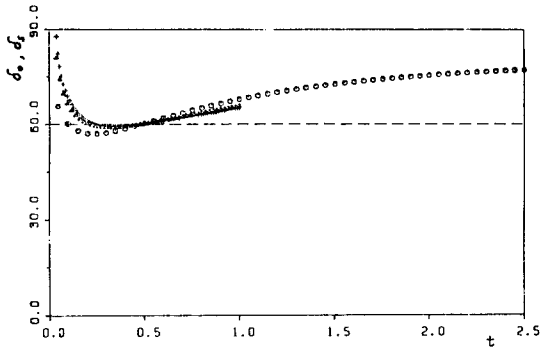

Fig. 9 Angles of the representative point vortices measured from the plate. ···δ_s by theory (14); symbols are numerical results of δ_0 by (25) for $h=0.25$. See the caption of Fig. 7 for classifications

is the numerical result. It is conjectured that as Δt is diecreased δ_o approaches δ_s.

In Fig. 10 is compared the form of vortex sheet depicted by the discrete model with that of the experimental observation. Similar pattern can be seen from this figure, although the scales for the two are not known.

5. Conclusions

The single vortex model is applied to obtain an approximate solution for the fluid motion around a semi-infinite flat plate impulsively started transversally. It turned out that the circulation increases like $O(t^{1/3})$, the distance between the plate edge and the vortex increases like $O(t^{2/3})$, and the angular position of the vortex is 60° with respect to the plate.

The numerical integration for the equations of the discrete vortices shows good agreement with

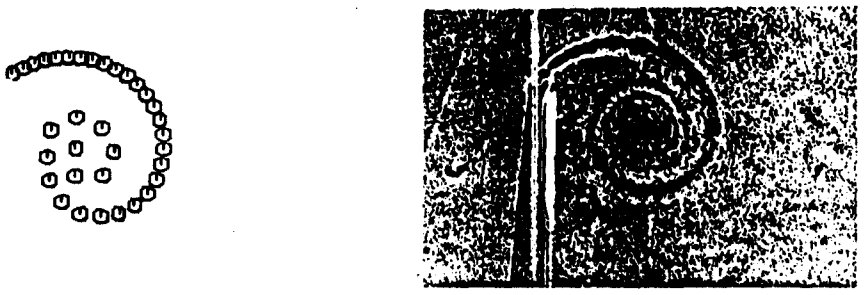

Fig. 10 Forms of vortex sheets depicted by (a) the discrete vortex model for $h=0.25$, $\Delta t=0.02$, by the second order method, and (b) the experimental observation excerpted from "an album of fluid motion" assembled by Van Dyke

the single-vortex solution. It also shows a similar pattern to the experimental evidence for the form of vortex sheet. Further study concerning the present investigation would be to apply a semi-analytic method to obtain a finer result than the discrete model. Extention could be made to the case in which the plate moves in power of t. Another extention is the similar motion around wedges.

References

1) Kiya, M., Sasaki, K. and M. Arie, "Discrete-Vortex Simulation of a Turbulent Separation Bubble", J. Fluid Mech., Vol. 120, pp. 219-244, 1982

2) Rosenhead, L., "The Formation of Vortices from a Surface of Discontinuity", Proc. Royal Soc. Lond., A134, pp. 170-192, 1931

3) Sarpkaya, T., "An Analytical Study of Seperated Fow about Circular Cylinders", J. Basic Eng., Dec. 1968, pp. 511-520, 1968

4) Chaplin, J. R., "Computer Model of Vortex Shedding from a Cylinder", J. Hyd. Div., Proc. Amer. Soc. Civ. Eng., HY1, Jan. 1973, pp. 155-165, 1973

5) Yang, H. T. and M. Bar-Lev, "Potential Flow Model for an Impulsively Started Circular Cylinder", J. Appl. Mech., Jun 1976, pp. 213-216, 1976

6) Stansby, P. K., "An Inviscid Model of Vortex Shedding from a Circular Cylinder in Steady and Oscillatory Far Flows", Proc. Instn. Engrs., Part 2, Vol. 63, pp. 865-880, 1977

7) Maull, D. J. and M. G. Milliner, "Sinusoidal Flow past a Circular Cylinder", Coastal Eng., Vol. 2, pp. 149-168, 1978

8) Kuwahara, K., "Study of Flow past a Circular Cylinder by an Inviscid Model", J. Phys. Soc. Jap., Vol. 45, pp. 292-297, 1978

9) Fink, P. T. and W. K. Soh, "Calculation of Vortex Sheets in Unsteady Flow and Applications in Ship Hydrodynamics", Proc. 10th Symp. Naval Hyd., Cam. Mass., pp. 463-488, 1974

10) Sarpkaya, T. S. and R. L. Schoaff, "Inviscid Model of Two-Dimensional Vortex Shedding by a Circular Cylinder", AIAA J., vol. 17, pp. 1193-1200

11) Higdon, J. J. and C. Pozrikidis, "The Self-Induced Motion of Vortex Sheets", J. Fluid Mech., Vol. 150, pp. 203-231, 1985

12) Merion, D. I., Baker, G. R. and S. A. Orszag, "Analytical Structure of Vortex-Sheet Dynamics", Part 1. Kelvin-Helmholz Instabillity, J. Fluid Mech., Vol. 114, pp. 283-298, 1982

13) Edwards, R. H. and H. K. Cheng, "The Seperation Vortex in the Weis Fogh Circulation-Generation Mechanism", J. Fluid Mech., Vol. 120, pp. 463-473, 1982

14) Durand, W. F., Aerodynamic Theory, Vol. Ⅱ, Div. E, pp. 320-326, 1943